Image analysis applied to electron micrographs of stirred yogurt

By ANNE SKRIVER*†, MARTIN B. HANSEN‡ and KARSTEN B. QVIST*

**Institute for Dairy Research and KVL Centre for Food Research, The Royal Veterinary and Agricultural University, Howitzvej 11, DK-2000 Frederiksberg, Denmark*

‡*Dina KVL, Department of Mathematics and Physics, The Royal Veterinary and Agricultural University, Thorvaldsensvej 40, DK-1871 Frederiksberg C, Denmark*

(*Received 9 March 1995 and accepted for publication 6 June 1996*)

Summary. An optimum or a high heat treatment of milk before yogurt preparation was applied according to an experimental design with the deliberate aim of making stirred yogurts with varying properties. Images of sections of yogurt samples were obtained using a transmission electron microscope. These were digitized and segmented via a threshold determination to separate the protein structure from the background. Four spatial statistical estimates were determined in order to evaluate their applicability for characterization of yogurt microstructure. The volume content was estimated and compared with the protein content obtained through chemical analysis. Heat treatment had no significant effect on volume content, as expected. The surface area of the protein aggregates was a useful measure to describe the difference between casein networks obtained by an optimum and a high heat treatment. The star volume gave a measure of the average local size of pores in the yogurt gel. The optimum heat treatment resulted in yogurt with small values for the star volume, indicating a less coarse structure of the casein network compared with yogurt prepared from high heat milk. The covariance function was able to differentiate between yogurts made using two types of heat treatment.

There have been many electron microscopy investigations involving descriptions of the microstructure of acid milk gels (Kalab *et al*. 1976; Harwalkar & Kalab, 1986; Tamime *et al*. 1989). Kalab *et al*. (1976) examined the microstructure of yogurt produced from heated and unheated skim milk. It was immediately apparent that the sizes of the casein aggregates were larger in the yogurt from unheated milk. This was quantified by measuring the mean diameter of 80 aggregates, and a significant difference between heated and unheated milk was confirmed. The mean size of casein aggregates in yogurts from unheated skim milk was twice that in yogurts from heated skim milk.

In contrast to milk, where the casein exists in individual micelles, rennet and acid milk gels form a continuous three dimensional network. This difference is relevant when analysing the microstructure. Quantitative information from micrographs of curd and cheese structure obtained by conventional transmission electron microscopy and light microscopy have been derived by Green *et al*. (1981), who described methods for assessing the fat–protein interfacial area from transmission

† Present address: Chr. Hansen A/S, Bøge Allé 10–12, DK-2970 Hørsholm, Denmark.

https://doi.org/10.1017/S0022029996001884 Published online by Cambridge University Press

electron micrographs and the coarseness of the protein matrix from light micrographs.

Bremer (1992) investigated the formation and properties of different particle gels (e.g. acid milk gels). Several models describing the formation of a gel were discussed and the fractal dimensionality (D) was determined. This explains how efficiently the flocs fill the available space. Computer simulations in spatial lattices have shown that $D = 1{\cdot}8$ if all collisions lead to attachment (diffusion-limited cluster–cluster aggregation; Meakin, 1984). In a spatial lattice Brown & Ball (1985) estimated $D = 2{\cdot}1$ if the sticking probability is very low (reaction-limited cluster–cluster aggregation). However, real life fractal dimensionalities may be higher owing to rearrangement of the flocs during aggregation. Bremer (1992) studied optical sections of acid sodium caseinate gels with casein concentrations from 16·2 to 40 g/kg by confocal laser scanning microscopy. Subsequently a correlation analysis of individual images was applied and estimates of D in the range 2·84–2·96 were obtained.

Steventon *et al*. (1991) studied gelation of whey protein concentrates by using percolation analysis. In this case the formation of gels was also simulated by computer calculation, but the approach was somewhat different. Here a number of particles were randomly distributed on a cubic lattice, and infinitely many connected particles were considered to be a network.

The objective of this research was to evaluate the applicability of some spatial statistical estimates to characterize a continuous isotropic three dimensional network from a two dimensional sectioned image. Further, the objective was to see how these values were influenced by different heat treatments of the milk before yogurt production.

Theory

Many global estimates can be determined on a sectioned image, including volume content, surface area, mean free distance between features and mean intercept length (Weibel, 1979; Russ, 1990). We chose to focus on the volume content of protein (V_V, %) and the surface content of protein per unit volume (S_V, mm^{-1}). By using Delesse's method (Weibel, 1979) an unbiased estimate of V_V can be obtained by calculating the area fraction A_A of protein in the two dimensional section. The surface density expresses the amount of surface area of the protein phase contained in a unit volume. A useful unbiased estimator for this quantity (Weibel, 1979) is obtained by multiplying the number of intersection points per unit length between the face of interest and the void, for a series of test lines drawn on the image.

Volume and surface estimation refer to the overall structure and do not attempt to describe the details of how the structure is organized. Description of this local organization is, however, important when one wishes to relate the structure to the rheological properties of the product. In the following we have chosen to focus on the star volume and the covariance function as descriptors of local features. Star volumes are a valuable tool to characterize pore size when identification of single particles or pores is inappropriate (Delfiner, 1972; Serra, 1982), and the covariance function describes the total spatial variation throughout the structure. Bremer (1992) calculated the correlation function (which is the covariance function scaled by the squared volume content) to characterize acid milk gels.

One way to define the star volume is to consider a given fixed point, and then measure the volume of the space which is visible from the fixed point, designated as the volume of a star at the point. If the structure is stationary the mean volume is

https://doi.org/10.1017/S0022029996001884 Published online by Cambridge University Press

independent of the fixed point and is denoted v^* and simply called the star volume (Serra, 1982). Direct calculation of v^* in a regular lattice is complicated and computer intensive, but if we assume isotropy there is a relationship between v^* and a density function of the linear distance from the fixed point to the phase in a given direction.

If the structure of interest is stationary and isotropically distributed, the covariance $C(r)$ between pixels separated by a distance r is defined as the probability that two given points positioned at a distance r both belong to the phase of interest (protein). Bremer (1992) has stated that the aggregation process leads to scale invariant network clusters. One way in which this fractal nature is often manifested is by a power-law behaviour of the covariance function (Bremer, 1992)

$$C(r) = \frac{D\,V_V^2}{3}\left(\frac{r}{a}\right)^{D-3}, \tag{1}$$

where D is the fractal dimensionality of the network, a is the particle radius and V_V is the volume content of the protein. Once $C(r)$ has been estimated, D can be assessed as the slope of a log–log plot of $C(r)\,v.\,r$. It is noticeable that this power law is valid over only a limited range because we get a lower cut-off as $C(0) = V_V$ and an upper cut-off as we would expect $\lim_{r\to\infty} C(r) = V_V^2$ due to independence at long distances. However, for particles scattered randomly throughout the solvent (e.g. as in the case of networks created by percolation (Steventon *et al.* 1991)), an exponentially decreasing covariance function would be expected (Stoyan *et al.* 1987)

$$C(r) = V_V(1-V_V)\exp(-\alpha r) + V_V^2, \tag{2}$$

where α denotes the amount of disorder and can be shown to be equal to $S_V/(4(1-V_V)\,V_V)$.

MATERIALS AND METHODS

Materials

Commercially homogenized and pasteurized whole milk (35 g fat/l) was purchased from a retail outlet. Spray-dried low heat skim milk powder from Akafa (DK-9230 Svenstrup) was used to raise the dry matter (DM) content of the milk samples. One superconcentrated commercial culture (DVS, Direct Vat Set) from Chr. Hansen A/S (DK-2970 Hørsholm; YC-180) consisting of *Streptococcus thermophilus* and *Lactobacillus delbrueckii* subsp. *bulgaricus* was used.

Yogurt preparation

Whole milk with the DM increased by 10 g/kg was heated to 85 °C and held for 10 or 30 min. After it was cooled to 43 °C, an inoculation of 0·2 g culture/kg was used. When the pH reached 4·4–4·3 the samples were vigorously stirred using a jet turbine mixer (Ystral X10/20 with a Y-formed mixer head; Ificon ApS, (DK-3600 Frederikssund) operating at high speed (110 V) for 1 min and cooled to 24 °C in an ice–water bath. After storage for 4 d at 5 °C, the yogurt was gently stirred in a standardized way and a sample was taken for electron microscopy.

Electron microscopy

The sampling was carried out by embedding the yogurt samples into agar as described by Schellhaass & Morris (1985). The agar cubes were fixed in glutaraldehyde (25 g l^{-1}) in 0·2 M-sodium cacodylate buffer, pH 7·2 and post fixed in osmium tetroxide (10 g l^{-1}) followed by three rinses in diluted cacodylate buffer (cacodylate–

https://doi.org/10.1017/S0022029996001884 Published online by Cambridge University Press

water, 1:1). After staining in uranyl acetate (5 g l^{-1}) and dehydration using an ethanol dehydration series, the samples were embedded in Epon, sectioned (75 nm) and stained with uranyl acetate (20 g l^{-1}) and lead citrate before examination in a Jeol-12 EX transmission electron microscope (Jeol AB, S-172 34 Sundbyberg, Sweden) operated at 60 kV. Micrographs were taken at two magnifications ($\times 5000$ and $\times 7500$; fields of view, $10{\cdot}0 \times 12{\cdot}5$ μm and $7{\cdot}5 \times 9{\cdot}4$ μm respectively) and all 48 were taken far apart to give independent replicates. For unbiased results the microscopic fields for photography were selected by moving the microscope table to a random position before looking into the microscope. The micrographs were digitized using a video camera connected to a personal computer.

Image analysis

Segmentation. Fig. 1(*a*) presents a typical example of a yogurt image from the microscope showing protein and fat globules. The corresponding histogram of the grey level distribution is also shown (Fig. 1*b*). Segmentation was based on brightness discrimination where a threshold level was established for each image. This was selected by a combination of interactive selection (where the user is allowed to look at the binary image as the settings are changed) and an automatic threshold (where the computer selects a minimum brightness value as threshold). A combination of the two methods was necessary, because manual selection alone was too subjective and probably gave biased results, and automatic threshold selection alone was inappropriate because the overall brightness level and contrast changed from image to image, owing to unavoidable variation in sample preparation and photography. This combination of two threshold techniques resulted in images with the same volume content (see Table 1), confirming that the results were independent of the overall brightness of the image. An erosion followed by a dilation was carried out in order to remove all small irrelevant objects (< 5 pixels) and to separate non-connected casein aggregates. A typical example of a segmented image is presented in Fig. 1(*c*).

Determination of estimates

We assumed that the casein aggregates were isotropically, randomly and uniformly distributed, because the product had been stirred and the direction of thin sectioning was random.

Volume estimation. V_V was estimated using Delesse's method (Weibel, 1979), determining the fraction of selected pixels in the segmented image. As the volume content is a ratio, the measurements were logit transformed to obtain a normally distributed expression.

Surface estimation. S_V of the casein aggregates was obtained by superimposing a test system of 15 line segments on each picture. A log transformation was performed in order to obtain a normally distributed expression.

Star volume. The value of v^* was estimated from the density function, which is easily computed by the number of pixels in a given direction between the fixed point and the phase of interest.

The covariance function. C(r) was calculated by template matching, performed by sliding the image across itself and counting how many pixels match per unit volume. To compensate for the different sizes represented by one pixel at the two magnifications, the values of r were multiplied by 1·5 for the images obtained at $\times 5000$. For each picture the covariance functions $\log(C(r) - V_V^2)$ and $\log(C(r))$ were plotted against the pixel distance r and $\log(r)$ respectively. Both plots were linear.

https://doi.org/10.1017/S0022029996001884 Published online by Cambridge University Press

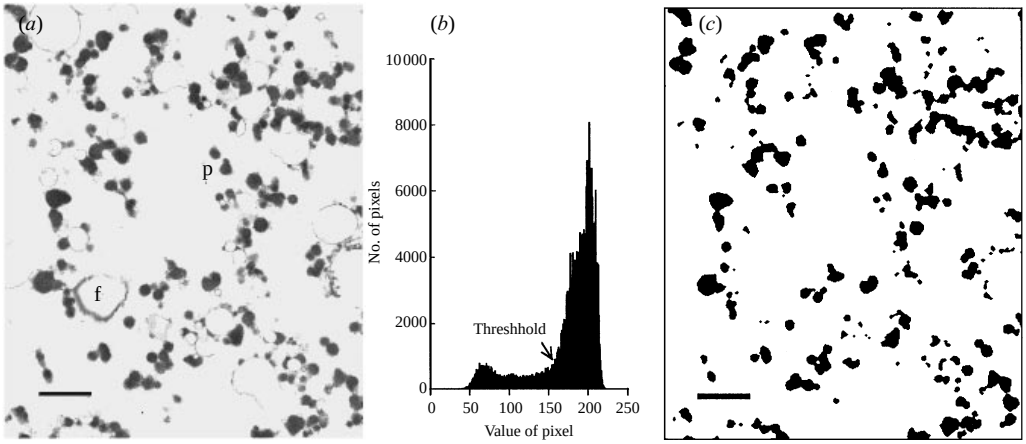


Fig. 1. (*a*) Electron microscopy image of yogurt (p, protein, f, fat globule), (*b*) the corresponding histogram and (*c*) the digital image segmented using a threshold at 160. Scale bar, 1 μm.

For the plot of $\log(\mathrm{C}(r) - V_{\mathrm{V}}^2)$ *v.* r, the slope α was calculated at distances r between 0 and 10 using eqn (2). For $\log(\mathrm{C}(r))$ *v.* $\log(r)$, D was calculated from r between 2 and 10 using eqn (1). The values of α and D were used for further analysis.

Experimental design and statistical analysis

The experimental design was laid out at a 2^2 factor experiment, with the treatment factor at two levels, optimum and high heat treatment and a block effect at two levels, $\times 5000$ and $\times 7500$ magnification (the magnifications were checked on the photographs). Twelve micrographs were taken of each combination (a total of 48 pictures).

The effects of heat treatment and magnification were determined by analysis of variance using the General Linear Model of the Statistical Analysis System program package (SAS, 1988), with the model

$$y_{ijk} = \mu + \alpha_i + \beta_j + (\alpha\beta)_{ij} + \epsilon_{ijk}, \tag{3}$$

where the ϵ_{ijk} were assumed to be normally distributed as $\mathrm{N}(0, \sigma^2)$ and independent. Here y_{ijk} is a statistic estimated for the ith heat treatment, jth magnification and kth image. The model was in each case verified by means of probit analysis in each group, and examination of the distribution of the residuals. The assumption of equal variance in each group was tested by a Bartlett test (Bartlett, 1937).

RESULTS

Typical examples of binary images of yogurt produced with varying heat treatment of the milk are presented in Fig. 2. Even though no rheological measurements were carried out, an organoleptic impression from stirring and oral perception showed that the viscosity of yogurt from optimum heat milk was higher than that from high heat milk.

The results from the analysis of variance for volume content, surface content, star volume, fractal dimensionality D and the slope α are shown in Table 1. For all the estimates no interaction effects between heat treatment and magnification were found. For the volume content there was no significant effect of the factors. The volume content estimate of the casein was 12·3 %.

https://doi.org/10.1017/S0022029996001884 Published online by Cambridge University Press

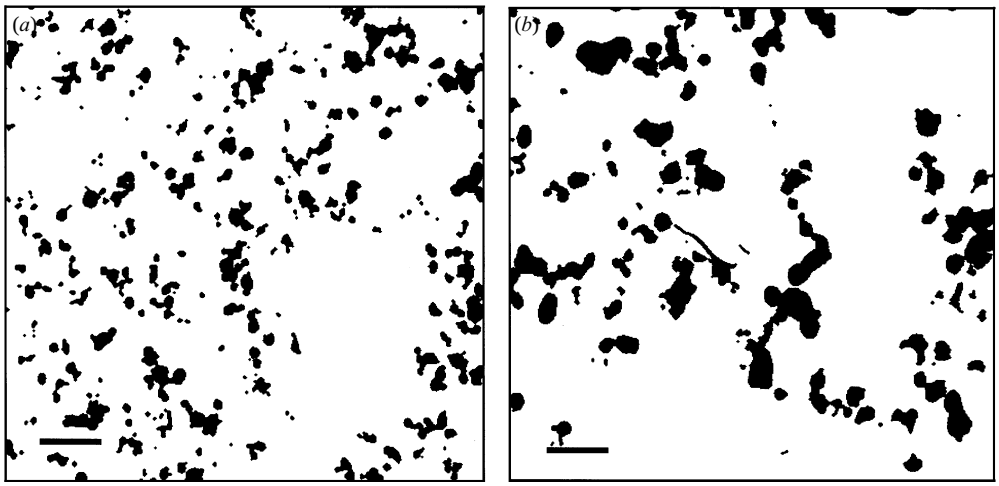


Fig. 2. Examples of segmented images obtained from micrographs of yogurt prepared from (*a*) optimum and (*b*) high heat milk. Scale bar, 1 μm.

Table 1. *Analysis of variance table and means for all estimated characteristics*

Characteristic	Magnification	Heat treatment	Mean	SE	*P* value†
Volume content	×5000		12·44 %	1·803	0·7638
	×7500			2·385	
		Normal		2·244	0·6085
		High		1·995	
Surface content	×5000		836·99 mm^{-1}	198·43	0·0149
	×7500		913·62 mm^{-1}	238·18	
		Normal	1082·92 mm^{-1}	119·55	0·0001
		High	704·45 mm^{-1}	109·47	
Star volume	×5000		980·91 μm^3	608·06	0·001
	×7500		508·57 μm^3	276·10	
		Normal	439·10 μm^3	238·48	0·0001
		High	1050·37 μm^3	557·27	
Fractal dimensionality (*D*)	×5000		2·8961	0·0111	0.0004
	×7500		2·9072	0·0156	
		Normal	2·8951	0·0142	0·0029
		High	2·9084	0·0117	
Slope (α)‡	×5000		−0·2620	0·0570	0·0022
	×7500		−0·2913	0·0761	
		Normal	−0·3361	0·0407	0·0001
		High	−0·2182	0·0264	

† *P* indicates the probability of obtaining a more extreme set of observations under the hypothesis of equal variables.

‡ α denotes the amount of disorder.

Surface content and star volume were both significantly influenced by both magnification and heat treatment. The highest magnification (×7500) resulted in higher surface content and lower star volume. The normal heated milk gave higher surface content and lower star volume.

The covariance explains the variation of the structure over a limited range. Typical examples of covariance functions are demonstrated in Fig. 3. It can be seen that the shapes of the curves depended on the heat treatment of the milk. As described earlier, *D* could be derived from the slope of the linear part, where fractal

https://doi.org/10.1017/S0022029996001884 Published online by Cambridge University Press

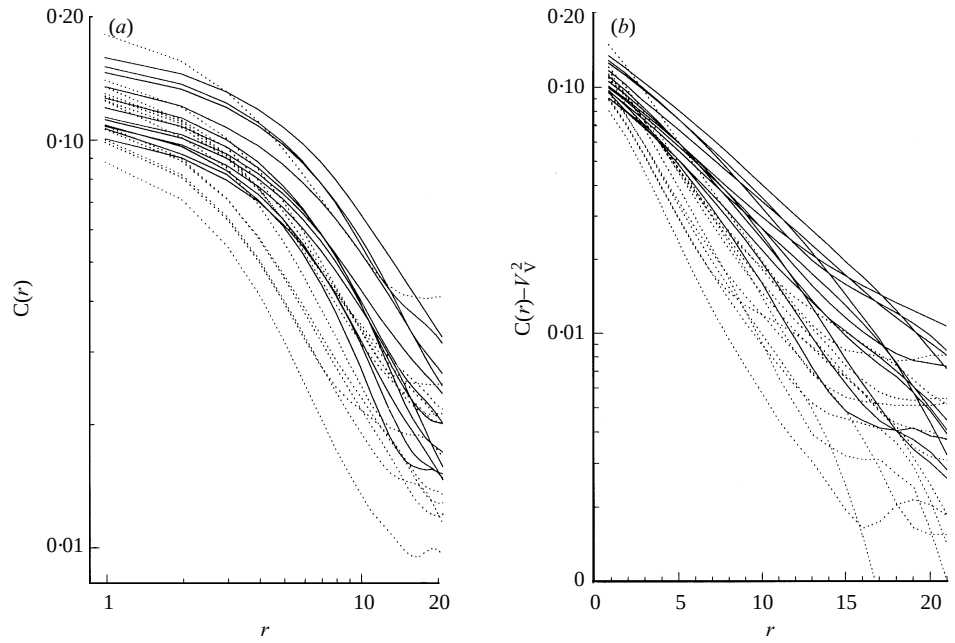


Fig. 3. Examples of covariance functions for magnification ×7500 at different scale types for ——, high heat; · · · · · · · · ·, optimum heat milk. r, Pixel distance; C(r), probability that two given points at a distance r both belong to the phase of interest (protein); V_V^2, square of volume content.

behaviour applies, in Fig. 3(*a*). An analysis of variance of D is shown in Table 1. There were significant effects of both magnification and heat treatment on D, indicating that the covariance function was a useful way to describe images of yogurt with varying microstructure properties. From Fig. 3(*b*) a good agreement with semi-log behaviour can be seen, especially for the yogurt from the high heat milk. The analysis of variance of the slope α (Table 1) showed significant effects for both heat treatment and magnification, again indicating the usefulness of the covariance function for discrimination between different types of microstructure.

DISCUSSION

From the volume content the voluminosity of the casein micelle could be calculated. As the weight of casein was 31 g l^{-1}, the voluminosity was 4 ml g^{-1}. This result falls within the range for native casein micelles obtained through different techniques (Walstra, 1979), but it may be fortuitous, as many factors influence the result.

The surface content was highly dependent on the heat treatment of the milk. By inspection of the images it seems that this difference could be explained by the sizes of the casein aggregates. The aggregates were larger in the yogurt from the high heat milk than in that from the optimum heat milk, leading to this difference in the surface content between the heat treatments. The high heat treatment resulted in a too extensive aggregation of the casein and consequently a lower surface content. The same effect can be seen for yogurt made from insufficiently heated or unheated milk (Kalab *et al.* 1976). The analysis clearly demonstrated that the method of estimating the surface content was able to differentiate between yogurts made from milk with varying heat treatment.

https://doi.org/10.1017/S0022029996001884 Published online by Cambridge University Press

The weakly significant effect of magnification on the surface content was probably caused by more details becoming visible at a higher magnification. An examination of the microstructure at many different magnifications would probably lead to a calculation of the fractal dimension.

The lower value of the star volume for the yogurt from optimally heated milk was related to a fine structure with many small pores compared with yogurt from high heat milk. The star volume would be expected to be related to the permeability of the gel and consequently to resistance to syneresis, which is an important technological characteristic.

The calculated D values were high (2·86–2·93) compared with the computer simulated values from different aggregation theories, as described in the introduction. However, Bremer (1992) estimated D from a correlation function and found values between 2·84 and 2·96 for sodium caseinate gels, depending on the particle concentration. Values of D higher than expected from simulations may be caused by rearrangements of flocs to a more compact configuration during aggregation. Moreover, the finite thickness of optical sections obtained with confocal laser scanning microscopy results in light from out of focus protein, which also gives higher D values. This effect was larger with the electron microscopy images obtained here, as the ratio between magnification and thickness of the section was lower. Further, it is not obvious that all the curves in Fig. 3(a) had a clear linear portion. This indicates that the presence of fractal aggregates created by cluster aggregation is questionable, and that it would be relevant to model the aggregation by other approaches. In the case of percolation (Fig. 3), the covariance function should decrease exponentially, thus giving a linear semi-log plot, and the fractal dimensionality should be 3.

From Fig. 3 it was not possible to decide whether cluster aggregation (leading to a linear section in the log–log plot) or percolation (leading to a linear portion in the semi-log plot) gave the better description of the formation of the protein network in yogurt. Even though both plots had linear sections for some of the samples, none of the models was completely satisfactory for all samples. This indicates that it is desirable to find a single model that can be used for all the yogurt samples. This would require further investigation.

In the present study we have chosen to work with binary images, which is conceptually easy, and a standard procedure. However, it should be noted that it is also possible to calculate the covariance (or correlation) function from the grey scale image (Bremer, 1992) and then let the grey scale value represent different densities of protein. This has the advantage of not requiring segmentation, but estimation of star volume and surface content is complicated.

From the above it seems that a few stereological estimates were sufficient to provide useful discrimination between different types of yogurt microstructure. Compared with the Bremer (1992) method, this was complicated by needing segmentation, but the estimates were easy to determine and the method was computerized, which made it useful for routine measurements of yogurt and related products.

We thank Bodil W. Jørgensen, José Bresciani and Pia S. Pedersen for assistance with the electron microscopy analysis and the Ministry of Agriculture for financial support.

https://doi.org/10.1017/S0022029996001884 Published online by Cambridge University Press

REFERENCES

Bartlett, M. S. 1937 Properties of sufficiency and statistical tests. *Proceedings of the Royal Society* A **160** 268–282

Bremer, L. 1992 *Fractal Aggregation in Relation to Formation and Properties of Particle Gels*. PhD thesis, Agricultural University, Wageningen

Brown, W. D. & Ball, R. C. 1985 Computer simulation of chemically limited aggregation. *Journal of Physics A* **18** L517–L521

Delfiner, P. 1972 A generalization of the concept of size. *Journal of Microscopy* **95** 203–216

Green, M. L., Turvey, A. & Hobbs, D. G. 1981 Development of structure and texture in Cheddar cheese. *Journal of Dairy Research* **48** 343–355

Harwalkar, V. R. & Kalab, M. 1986 Relationship between microstructure and susceptibility to syneresis in yoghurt made from reconstituted nonfat dry milk. *Food Microstructure* **5** 287–294

Kalab, M., Emmons, D. B. & Sargant, A. G. 1976 Milk gel structure. V. Microstructure of yoghurt as related to the heating of milk. *Milchwissenschaft* **31** 402–408

Meakin, P. 1984 Diffusion-limited aggregation in three dimensions. Results from a new cluster–cluster aggregation model. *Journal of Colloid and Interface Science* **102** 491–504

Russ, J. C. 1990 *Computer-Assisted Microscopy*. New York: Plenum

SAS 1988 *SAS/STAT™ User's Guide*, Release 6.03 Cary, NC: SAS Institute

Schellhaass, S. M. & Morris, H. A. 1985 Rheological and scanning electron microscopic examination of skim milk gels obtained by fermentating with ropy and non-ropy strains of lactic acid bacteria. *Food Microstructure* **4** 279–287

Serra, J. 1982 *Image Analysis and Mathematical Morphology*, vol. 1. London: Academic Press

Steventon, A. J., Gladden, L. F. & Fryer, P. J. 1991 A percolation analysis of the concentration dependence of the gelation of whey protein concentrates. *Journal of Texture Studies* **22** 201–218

Stoyan, D., Kendall, W. S. & Mecke, J. 1987 *Stochastic Geometry and Its Applications*. Chichester: Wiley

Tamime, A. Y., Kalab, M. & Davies, G. 1989 Rheology and microstructure of strained yoghurt (labneh) made from cow's milk by three different methods. *Food Microstructure* **8** 125–135

Walstra, P. 1979 The voluminosity of bovine casein micelles and some of its implications. *Journal of Dairy Research* **46** 317–323

Weibel, E. R. 1979 *Stereological Methods*, vol. 2. London: Academic Press

https://doi.org/10.1017/S0022029996001884 Published online by Cambridge University Press